

Post-exposure protection of SARS-CoV-2 lethal infected K18-hACE2 transgenic mice by neutralizing human monoclonal antibody

Ronit Rosenfeld*, Tal Noy-Porat, Adva Mechaly, Efi Makdasi, Yinon Levy, Ron Alcalay, Reut Falach, Moshe Aftalion, Eyal Epstein, David Gur, Theodor Chitlaru, Einat B. Vitner, Sharon Melamed, Boaz Politi, Ayelet Zauberman, Shirley Lazar, Yentl Evgly, Shmuel Yitzhaki, Shmuel C. Shapira, Tomer Israely and Ohad Mazor*

Israel Institute for Biological Research, Ness-Ziona, Israel

* Address correspondence to:

Ronit Rosenfeld; Ohad Mazor

Israel Institute for Biological Research

Ness-Ziona 74100, Israel

E-mail: ronitr@iibr.gov.il; ohadm@iibr.gov.il

Abstract

Coronavirus disease 2019 (COVID-19) pandemic, caused by the severe acute respiratory syndrome coronavirus 2 (SARS-CoV-2), exhibits high levels of mortality and morbidity and has dramatic consequences on human life, sociality and global economy. Neutralizing antibodies constitute a highly promising approach for treating and preventing infection by this novel pathogen. In the present study, we characterized and further evaluated the recently identified human monoclonal MD65 antibody for its ability to provide protection against a lethal SARS-CoV-2 infection of K18-hACE2 transgenic mice. 75% of the untreated mice succumbed 6-9 days post-infection while administration of the MD65 antibody as late as 3 days after exposure, rescued all infected animals. The data unprecedentedly demonstrate, the therapeutic value of human monoclonal antibodies as a life-saving treatment of severe COVID-19 infection.

Introduction

Human monoclonal antibodies (mAbs), specifically targeting surface viral proteins, have increasingly demonstrated prophylactic and therapeutic efficacy against various viruses including HIV, Ebola, and the pathogenic beta-coronaviruses MERS-CoV and SARS-CoV¹⁻⁵. Neutralizing antibodies constitute a highly promising approach for treating and preventing infection by the novel SARS-CoV-2⁶. The viral surface spike glycoprotein, is essential for viral attachment, fusion and entry into human cells and thus considered as the major target for therapeutic neutralizing antibodies⁷⁻¹³. Specifically, highly potent neutralizing antibodies target and block the binding of the receptor binding domain (RBD) located in the S1 subunit of the spike, to the human angiotensin-converting enzyme 2 (hACE2)^{7,10,14}.

A reliable animal model for COVID-19, is essential for the development of anti-SARS-CoV-2 countermeasures and for deciphering the pathogenicity of the disease¹⁵. Accordingly, mouse models that exploit the recombinant hACE2 expression, either by transgenic or viral-transduction approaches were developed¹⁶⁻²⁷. A transgenic mouse strain expressing hACE2 under the K18 promoter (K18-hACE2) was shown to be highly susceptible to SARS-CoV-2 infection, resulting in significant viral load in the lungs, heart, brain and spleen as well as mortality^{26,27}. In response to the urgent need for antibody-based therapy for COVID-19, several reports have demonstrated efficacy against SARS-CoV-2 infection by neutralizing antibodies, primarily as prophylactic protection^{10,19,28-30}. These studies were based on non-lethal COVID-19 models of mice transduced to express hACE2, and did not demonstrate the efficacy of Ab-based passive therapy administered at a significant time post-infection.

We have previously reported the isolation of human neutralizing Abs selected against SARS-CoV-2 RBD by extensive screening of a phage-display library generated from lymphocytes collected from infected individuals. Among these Abs, MD65 exhibited the highest neutralization potency *in vitro*¹¹. The aim of the current study was to evaluate the therapeutic efficacy of this Ab in a lethal COVID-19 animal model by assessing its prophylaxis and treatment abilities to protect K18-hACE2 infected mice.

Results and Discussion

Reformatting and characterization of the MD65 antibody. The initial binding and neutralization characterization of MD65 Ab were conducted following the expression of this antibody as a single-chain human- Fc recombinant form (scFv-Fc)¹¹. Here, towards implementation of this antibody as a *bona-fide* therapeutic product appropriate for human use, it was re-cloned and produced as a full recombinant IgG molecule of the IgG1/k isotype which includes the triple mutation M252Y/S254T/T256E (YTE) in the Fc region. These modifications increase the antibody affinity towards the human FcRn³¹ at acidic pH and thereby prolong its serum half-life, a parameter that is essential for a high therapeutic value³²⁻³⁴. Characterization of three versions of the MD65 Ab: scFv-Fc, IgG and IgG-YTE, established that overall they are highly comparable with regard to their antigen-binding performance (Fig. 1a) and that the IgG versions exhibit slightly favorable affinity when compared to the scFv-Fc one (apparent K_D of 0.7 nM versus 1.0 nM, respectively). Similarly, the two MD65 IgG formats possess equivalent SARS CoV-2 neutralization potency *in vitro* (NT₅₀ of 40 ng/ml) which is slightly better than that of the scFv-Fc antibody (NT₅₀ of 67 ng/ml; Fig. 1b). In addition, all three Ab versions were shown to effectively prevent the binding of SARS-CoV-2 spike RBD to the hACE2, again with favorable kinetics for the IgG formats (Fig. 1c). These slight differences may indicate that there is a correlation between antibody affinity and SARS CoV-2 neutralization. This aspect will be further clarified in future studies.

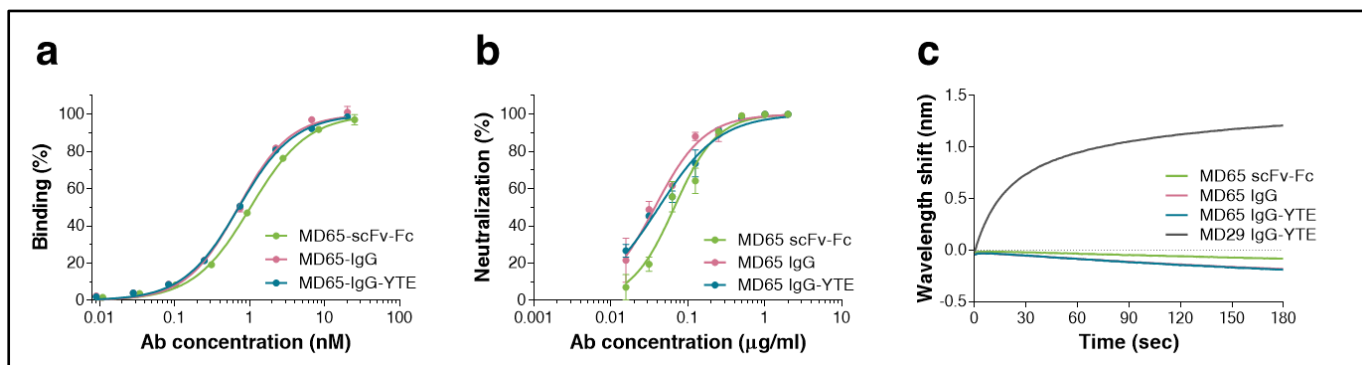


Fig.1 Characterization of the MD65 Ab versions. **a** Binding profiles of MD65 Ab variants, tested by ELISA against S1. Values along the curve, depict averages of triplicates \pm SEM. **b** SARS-CoV-2 *in vitro* neutralization potency of the MD65 Ab variants evaluated by plaque reduction neutralization test (PRNT). Values are averages of triplicates \pm SEM. **c** BLI-determined binding of hACE2 to RBD in the presence of MD65 Ab variants or MD29 IgG-YTE (as a control). Each of the biotinylated antibodies was immobilized on a streptavidin sensor, saturated with RBD, washed and incubated with recombinant hACE2 for 180 sec. Time 0 represents the binding of the hACE2 to the antibody-RBD complex.

Pharmacokinetics of MD65 IgG-YTE. A pre-requisite for achieving long circulatory half-life of a given antibody in humans, is to improve its interaction with the FcRn at low pH. We therefore verified that MD65 in its IgG-YTE format, as anticipated, exhibits improved pharmacokinetic abilities compared to the WT IgG format. Accordingly, the interactions of MD65 IgG and IgG-YTE with human FcRn, at pH 6.0 were assessed by biolayer interferometry (BLI). As expected, the modified antibody demonstrated a marked increase in affinity compared to the non-modified version, manifested by a three-fold improved *on*-rate and significant lower *off*-rate of binding (Fig. 2a and b). Steady-state analysis of these interactions revealed that the overall affinity of the IgG-YTE version toward human FcRn at low pH is 10-fold higher than the IgG version (Fig. 2c).

As part of the pre-clinical evaluation of MD65 IgG-YTE antibody and prior to the examination of its therapeutic potency in K18-hACE2 mice, we determined the pharmacokinetic profile following intravenous (IV) or intraperitoneal (IP) administration. Accordingly, MD65 IgG-YTE was first intravenously injected to K18-hACE2 mice and plasma antibody levels at various time points were determined by ELISA. The data were fitted by non-linear regression, establishing that MD65 IgG-YTE exhibits a biphasic elimination profile (Fig. 2d), consisting of a typical relatively short distribution phase (α) with a $t_{1/2}$ value of about 180 min and a significantly longer

elimination phase (β) with a $t_{1/2}$ value of about 4,700 min (3.3 days; Fig. 2f). These results are in good agreement with our previous observation that a chimeric protein bearing the same Fc (non YTE) exhibited similar pharmacokinetic parameters in mice³⁵, corroborating the notion that these mutations do not affect the antibody interaction with the murine FcRn.

The plasma levels of MD65 IgG-YTE following IP administration was then evaluated. The antibody exhibited a rapid and high bioavailability, reaching C_{max} of 40 $\mu\text{g/ml}$ within 180 min, which is similar to its sera concentration at the same time point as observed following the IV-administration (Fig. 2e). The elimination phase $t_{1/2}$ value following IP administration was approximately 5300 min (3.7 days; Fig. 2f). Therefore, the pharmacokinetic evaluation of the two alternative routes of administration indicate that they both are appropriate for the subsequent protection studies.

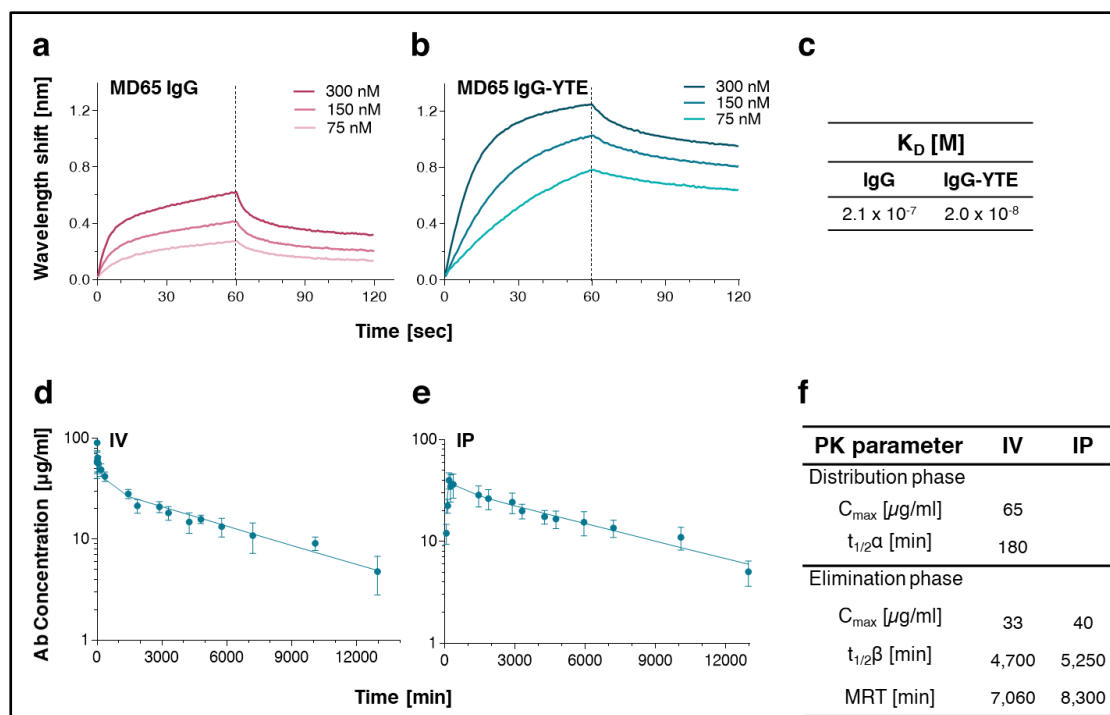


Fig. 2 MD65 binding to human FcRn and pharmacokinetic analysis. **a** and **b** Kinetics of the interactions between human FcRn and MD65 variants (**a** IgG; **b** IgG-YTE) at pH 6.0, using BLI. Immobilized antibodies were interacted with the indicated concentrations of human FcRn for 60 sec (association phase) followed by a wash step (dissociation phase). **c** Steady-state analysis of sensorgrams by 1:1 binding model was used to determine equilibrium K_D . **d** and **e** Plasma MD65 IgG-YTE concentrations in K18-hACE2 mice were determined at the indicated time points following a single (**d**) IV (n=4) or (**e**) IP (n=5) administration of 0.2 mg Ab. Values are expressed as mean \pm SEM that were fitted using non-compartmental analysis. **f** Pharmacokinetic parameters of MD65 IgG-YTE.

Protection against SARS-CoV-2 lethal infection in K18-hACE2 transgenic mice.

To directly assess the use of the MD65 antibody as the basis for pre- and post-exposure therapy to countermeasure the SARS-CoV-2 infection, the K18-hACE2 transgenic murine model, was employed for *in vivo* neutralizing studies. This model was recently shown to fatefully recapitulate the SARS-CoV-2 infection and consequently to serve as a reliable model to predict the efficacy of therapeutic strategies^{18,26 27,36}.

Infection of K18-hACE2 mice with 200 PFU of the SARS-CoV-2 BavPat1/2020 strain, resulted in massive weight loss from day 5 after infection and death of 75% of the animals at days 6 to 9 post infection (Fig. 3b and 3c).

In order to maintain a steady antibody levels in the circulation for about 8 days (the mean time to death in the control group), and taking into consideration the pharmacokinetic profile of the antibody, it was administered via the IP route in two successive treatments, 4 days apart. In sharp contrast to mock-treated mice (administered with PBS only), pre-exposure IP-administration of the MD65 antibody 4 h before infection (first dose) resulted in full protection of the infected animals without any signs of weight loss (Fig. 3b and 3c) or any other clinical symptoms. The high lethality of the infection could not be alleviated in mice administered with an isotype antibody control (MH75) that contains the same Fc but targets a non-relevant antigen (ricin)³⁷.

The successful pre-exposure treatment of the infected mice prompted us to further evaluate the possibility to initiate treatment at even later time-points. K18-hACE2 mice were therefore infected with SARS-CoV-2 and IP-administered (first dose) with the MD65 antibody 1, 2, 3 or 4 days post-infection (dpi). It was found that treatment of infected mice initiated as late as 2 days after infection, was highly efficient in blocking the disease, as demonstrated by the complete prevention of weight loss and, most notably, by total protection of the mice (Fig. 3d and 3e). Furthermore, even when treatment was initiated 3 dpi, all treated animals survived. Yet, mice in this experimental group displayed some mild symptoms during the first 10 dpi, as manifested by moderate delay in the gain of weight, compared to the non-infected naive animals. Further delaying the treatment to 4 dpi resulted in a protection rate of 60% of the infected animals without a significant delay in the time to death (for the non-surviving animals). Taken together, these results demonstrate, for the first time, the therapeutic value of human monoclonal antibodies as a life-saving treatment of severe and lethal COVID-19 infection model.

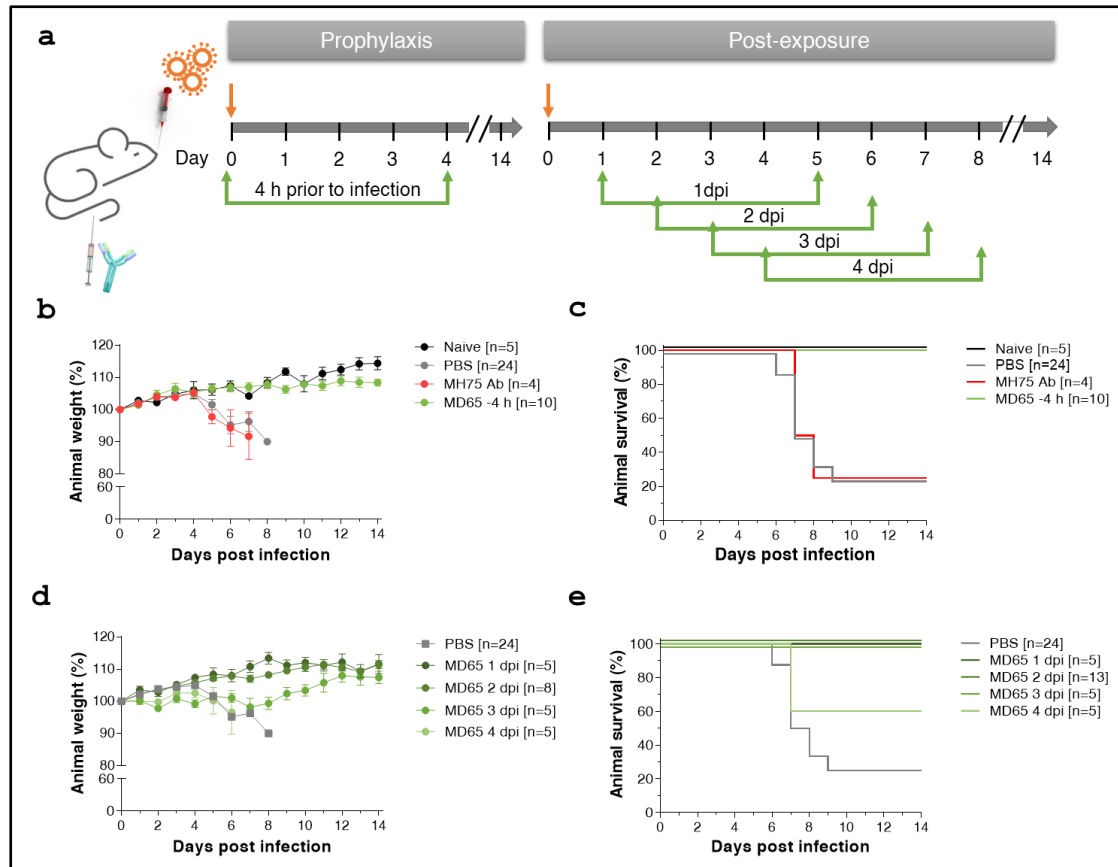


Fig. 3 MD65 Ab prophylactic and post-exposure protection against SARS-CoV-2 infected K18-hACE2 mice. **a** Schematic description of the prophylactic (left) or post-exposure (right) experimental design of the *in vivo* protection experiments. Animals were intranasal-infected with 200 PFU of SARS-CoV-2 BavPat1/2020 strain and IP-administered with 1 mg/mouse of MD65 Ab at the indicated time points and for a second time, 4 days later. **b** and **c** Prophylactic treatment experiment. Body weight profiles (**b**) and Kaplan-Meyer surviving curves (**c**). Curves describe naïve untreated and un-infected animals (black line), control animals which were initially administered 4 h prior to the infection either with PBS (grey line) or with 1 mg/mouse of isotype control irrelevant-Ab (anti ricin MH75; red line). **d** and **e** Post-exposure treatment experiment. Body weight profiles (**d**) and Kaplan-Meyer surviving curves (**e**). Same curve describing the control PBS-administered mice as in **b** and **c** is included (grey line). Body weight change is displayed as percentage of initial weight (only data of the first 6-8 days is presented in the groups exhibiting significant mortality). Data represent means \pm SEM and compiled from 4 independent experiments.

Anti SARS CoV-2 seroconversion in antibody-treated animals. It was previously shown that following passive immunization, animals that survived the pathogen challenge seroconverted by developing antigen-specific antibodies, in correlation with protection against re-infection³⁸. More specifically, in the case of the current pandemic, where the re-infection by SARS-CoV-2 is a tangible possibility, it was of interest to determine whether the MD65-treated mice developed an endogenous immune response toward the virus. To this objective, the mouse humoral immune response towards SARS-CoV-2 Spike glycoprotein was measured in treated mice at 14 dpi. Interestingly, the prophylactic administration of the MD65 Ab prevented the mounting of the humoral response, suggesting that effective neutralization of the virus occurred immediately upon infection (Fig. 4a). In contrast, animals treated either 1- or 2-days post-infection developed a marked antibody response that is in good correlation with the time of treatment. As several studies have shown that most SARS-CoV-2 neutralizing antibodies target the S1 subunit and even more specifically the RBD, the humoral responses of the antibody-treated mice toward these two antigens was further evaluated. Indeed, a similar pattern was observed for these two antigens as for the spike (Fig. 4b and 4c), suggesting that the endogenous antibody response may contain SARS-CoV-2 neutralizing antibodies that will confer partial or full protection against re-infection. Determination of the neutralization titer of these samples could provide further support for this concept, yet such an experiment is complicated by the masking effect of residual MD65 Ab.

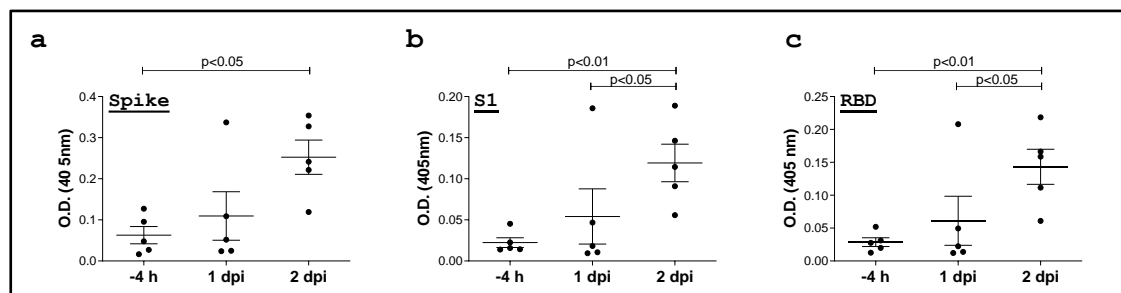


Fig. 4 Endogenous anti-SARS-CoV-2 humoral response in mice. Sera samples were collected at day 14 post-infection from the indicated antibody treated groups (as in Figure 3, n=5) and tested by ELISA for the presence of endogenous (murine) antibodies against the SARS-CoV-2 antigens: (a) spike, (b) S1 or (c) RBD. Data represent individual and mean \pm SEM (n=5 mice) of measurements obtained for sera samples at 1:60 dilution. Horizontal bars indicate statistical significance of paired values.

Antibody dependent enhancement (ADE) of infection was documented for several viruses including respiratory syncytial virus (RSV), measles as well as for corona viruses³⁹. This phenomenon is usually associated with the enhancement of virus uptake by phagocytic cells or by the formation of immune complexes that lead to excessive inflammatory responses. Post-exposure treatment of infected animals, where the possibility for the formation of immune-complexes is higher, was proposed as one of the tests for possible ADE effects in general and of SARS CoV-2 in particular³⁹. As of today, ADE was not reported for the current pandemic, yet there is a need to continue monitoring for such effect {Arvin, 2020 #221. In the current study, no worsened effect in the antibody treated animals was observed, in spite of the high sensitivity of the K18-hACE2 model which could have detected with ease such an occurrence.

To conclude, the data presented in this report demonstrates for the first time, to the best of our knowledge, high-effective post-exposure therapy of SARS-CoV-2 lethal infection in an animal model using a fully human monoclonal antibody. From the clinical point of view, the efficacy of this antibody extends the therapeutic window permitting initiation of life-saving treatment at late stages post-infection. This study incents the development of a clinical product based on the MD65 antibody for human use.

Methods

Recombinant proteins expression

Mammalian cell codon optimized nucleic sequence, coding for the SARS-CoV-2 Spike glycoprotein [GenPept: QHD43416 ORF (<https://www.ncbi.nlm.nih.gov/protein/1791269090>)], was used to design pcDNA3.1⁺ based expression plasmids, mediating recombinant expression of the soluble spike (amino acids 1-1207), S1 (amino acids 1-685) and RBD (amino acids 1–15 and 318–542) proteins. Same expression vector utilized for cloning and production of the secreted form of the human angiotensin-converting enzyme 2 (ACE2) receptor [amino acids 1-740; GenPept: NP_068576.1 ORF (https://www.ncbi.nlm.nih.gov/protein/NP_068576.1)]. C-terminal his-tag as well as a strep-tag, were included in order to facilitate protein purification. Expression of the recombinant proteins was performed using ExpiCHOTM Expression system (Thermoscientific, USA, Cat# A29133) following purification using HisTrapTM (GE Healthcare, UK) and Strep-Tactin@XT (IBA, Germany).

MD65 scFv, derived from a phage-display library, was initially cloned as a scFv-Fc Ab, as recently described¹¹. To generate a full-length IgG, the VH and VL fragments were re-cloned into pcDNA3.1-Heavy and pcDNA3.1-Kappa vectors, respectively. These vectors, were designed in to include IgG1 and Kappa chain constant domains, as well as the appropriate signal sequences for the production of complete heavy and light chains. The resulting antibody was further engineered to include three point mutations in its Fc region: M252Y/S254T/T256E (YTE mutations). These mutations were previously shown to increase antibody affinity to the human FcRn, at pH 6.0 and hence, to improve the Ab's serum half-life in rhesus macaques and humans^{31,33,34}. The antibody MD29 scFc-Fc, reported to target RBD and neutralize SARS-CoV-2 but not inhibit ACE2-RBD interaction¹¹, was similarly cloned and expressed as IgG-YTE.

Recombinant antibodies (scFv-Fc, IgG and IgG-YTE) were expressed using ExpiCHOTM Expression system (Thermoscientific, USA, Cat# A29133) and purified on HiTrap Protein-A column (GE healthcare, UK).

All purified proteins were sterile-filtered and stored in PBS. The integrity and purity of the recombinant expressed proteins were confirmed by SDS-PAGE analysis (Supplementary Figure 1).

ELISA

Direct ELISA was performed against SARS-CoV-2 S1 subunit (expressed and purified as recently described¹¹) for binding evaluation and for Ab concentration determination. Maxisorp 96-well microtiter plates (Nunc, Roskilde, Denmark) were coated overnight with 1 µg/ml of S1 protein in NaHCO₃ buffer (50 mM, pH 9.6), washed, and blocked with PBST at room temperature for 1 h. Human Abs were visualized by AP-conjugated Donkey anti-human IgG (Jackson ImmunoResearch, USA, Cat# 709-055-149, lot 130049) used at 1:1,000 and further developed with PNPP substrate (Sigma, Israel, Cat# N1891). For the quantification of MD65 Ab presence in plasma or sera samples, standard curve included purified MD65 IgG-YTE Ab at the concentration range of 2-3000 ng/ml (diluted in PBST) was used. Correct ELISA-based quantification was confirmed by 4 non-immune sera samples (collected prior to Ab-administration) containing exogenously-added known concentration of the Ab. Standard curve confirmed as above, were calculated for each individual ELISA plate/data set.

The endogenous humoral response was tested in mice sera samples collected at 14 dpi, evaluated by ELISA against SARS-CoV-2 spike, S1 and RBD essentially as described above, using AP-conjugated Donkey anti-mouse IgG (H+L) minimal cross (Jackson ImmunoResearch, USA, Cat# 715-055-150, lot 142717) used at 1:2,000.

Biolayer interferometry (BLI) analysis

Binding studies were carried out using the Octet system (ForteBio, USA, Version 8.1, 2015) which measures biolayer interferometry (BLI). All steps were performed at 30°C with shaking at 1,500 rpm in a black 96-well plate containing 200 µl solution in each well. For hACE2 competitive binding assay, streptavidin-coated biosensors were loaded with biotinylated MD65 (10 µg/ml), as either scFv-Fc, IgG or IgG-YTE antibody formats. Antibody-loaded sensors were first incubated with RBD (12 µg/ml), washed and incubated with hACE2 (20 µg/ml). MD29 Ab, previously shown to bind RBD without blocking its binding to hACE2¹¹, was used as a control.

For the evaluation of MD65 affinity to human FcRn, anti-Fab coated sensors were loaded with MD65 IgG or IgG-YTE (30 µg/ml), to reach 2.5 nm wavelength shift, and then washed. Sensors were then incubated with different concentrations of FcRn (Sino Biological #CT009-H08H; ranging from 75 to 300 nM) in pH 6.0, for 60 sec (association phase) and transferred to buffer-containing wells for additional 60 sec (dissociation phase). Binding and dissociation were measured as changes over time in

light interference after subtraction of parallel measurements from unloaded biosensors. Sensorgrams were fitted with a 1:1 binding model using the Octet data analysis software 8.1 (Fortebio, USA, 2015). All BLI experiments were repeated several times.

Cells

Vero E6 (ATCC® CRL-1586™) were obtained from the American Type Culture Collection. Cells were grown in Dulbecco's modified Eagle's medium (DMEM) supplemented with 10% fetal bovine serum (FBS), MEM non-essential amino acids (NEAA), 2 mM L-Glutamine, 100 Units/ml Penicillin, 0.1 mg/ml Streptomycin and 12.5 Units/ml Nystatin (P/S/N) (Biological Industries, Israel). Cells were cultured at 37°C, 5% CO₂ at 95% air atmosphere.

ExpiCHO-S (Thermoscientific, USA, Cat# A29127) were used for expression of recombinant proteins as described above.

Plaque reduction neutralization test (PRNT)

Handling of SARS-CoV-2 was conducted in a BSL3 facility in accordance with the biosafety guidelines of the Israel Institute for Biological Research (IIBR). SARS-CoV-2 (GISAID accession EPI_ISL_406862) strain was kindly provided by Bundeswehr Institute of Microbiology, Munich, Germany. Virus stocks were propagated and tittered by infection of Vero E6 cells as recently described⁴⁰. For plaque reduction neutralization test (PRNT), Vero E6 cells were plated overnight (as detailed above) at a density of 5×10^5 cells/well in 12-well plates. Antibody samples were 2-fold serially diluted (ranging from 2 to 0.015 µg/ml) in 400 µl of MEM supplemented with 2% FBS, NEAA, 2 mM L-Glutamine and P/S/N. 400 µl containing 500 PFU/ml of SARS-CoV-2 virus were then added to the Ab solution supplemented with 0.25% guinea pig complement sera (Sigma, Israel) and the mixture incubated at 37°C, 5% CO₂ for 1 h. Monolayers were then washed once with DMEM w/o FBS and 200 µl of each Ab-virus mixture was added in triplicates to the cells for 1 h. Virus mixture w/o Ab was used as control. 2 ml/well overlay [MEM containing 2% FBS and 0.4% Tragacanth (Sigma, Israel)] were added to each well and plates were further incubated at 37°C, 5% CO₂ for 48 h. Following incubation, the overlay was aspirated and the cells were fixed and stained with 1 ml of crystal violet solution (Biological industries, Israel). The number of plaques in each well was scored and the NT₅₀ (Ab concentration at which the plaque number was reduced by 50%, compared to plaque number of the control, in the absence

of Ab), was calculated using the Prism software version 8 (GraphPad Software Inc., USA).

Animal experiments

Treatment of animals was in accordance with regulations outlined in the U.S. Department of Agriculture (USDA) Animal Welfare Act and the conditions specified in the Guide for Care and Use of Laboratory Animals (National Institute of Health, 2011). Animal studies were approved by the local ethical committee on animal experiments (protocol number M-51-20 and M-56-20). Male and female outbred K18-hACE2 transgenic and C57BL/6 mice (Jackson Laboratories, USA) were maintained at 20–22 °C and a relative humidity of 50 ± 10% on a 12 h light/dark cycle, fed with commercial rodent chow (Koffolk Inc.) and provided with tap water *ad libitum*. All animal experiments involving SARS-CoV-2 were conducted in a BSL3 facility.

Infection experiments were carried out using SARS-CoV-2, isolate Human 2019-nCoV ex China strain BavPat1/2020 that was kindly provided by Prof. Dr. Christian Drosten (Charité, Berlin) through the European Virus Archive – Global (EVAg Ref-SKU: 026V-03883). Virus was propagated and tittered by infection of Vero E6 cells.

SARS-CoV-2 BavPat1/2020 virus diluted in PBS supplemented with 2% FBS (Biological Industries, Israel) was used to infect animals by intranasal instillation of anesthetized mice. For Abs protection evaluation, mice were treated with 4 days interval double dose of 1 mg/mouse of MD65 Ab first administered IP either 4 h prior, 1 or 2 days post-infection with 200 PFU of SARS-CoV-2. Control groups were administered 4 h prior to infection with PBS or isotype control Ab (anti ricin MH75 Ab). Animals' body weight was monitored daily over 5 or 14 days. Mice were evaluated once a day for clinical signs of disease and dehydration.

Pharmacokinetics

Pharmacokinetics was determined in male and female outbred K18-hACE2 transgenic and C57BL/6 mice following administration of 0.2 mg MD65 IgG-YTE Ab either by intravenous (IV; n=4; 200 µl of 1 mg/ml Ab) or intraperitoneal [IP; n=5; 1 ml of 0.2 mg/ml Ab] route. At different time points, 5 µl blood samples were drawn from the tail vein, diluted 20-fold in PBS, and centrifuged for 10 min at 500 g for the removal of red blood cells. Supernatant plasma fractions were stored at -20°C until tested in ELISA

for the Ab concentration determination as described above. Average antibody concentration at each time point was used for calculating the pharmacokinetic parameters using non-compartmental analysis (PK solutions 2.0, Summit Research Services, USA).

Data and materials availability

All data are available from the corresponding authors upon reasonable request. Antibody is available (by contacting Ohad Mazor from the Israel Institute for Biological Research; ohadm@iibr.gov.il) for research purposes only under an MTA, which allows the use of the antibody for non-commercial purposes but not its disclosure to third parties.

Acknowledgments

We thank Prof. Dr. Christian Drosten at the Charité Universitätsmedizin, Institute of Virology, Berlin, Germany for providing the SARS-CoV-2 BavPat1/2020 strain. We wish to express our gratitude to our colleagues Dr. Hagit Achdout, Dr. Nir Paran, Dr. Emanuelle Mamroud, Dr. Hadas Tamir, Dr. Yfat Yahalom-Ronen, Dr. Shay Weiss, Dr. Hadar Marcus, Dr. Noa Madar-Balakirski, Roy Avraham, Dr. Amir Rosner and Dr. Tseela David for fruitful discussions and support. We would like to thank Moshe Mantzur, Tamar Aminov, Meni Girshengorn and Sarah Borni for skillful and devoting technical assistance.

Author Contributions

R.R., T.N-P., A.M., E.M., Y.L., R.A., R.F., M.A., E.E., D.G., E.B.V., S.M., B.P., A.Z., S.L., Y.E. and O.M. designed, carried out and analyzed the data. T.C., S.Y., S.S and T.I. added fruitful discussions, reviewed and edited the manuscript. R.R. and O.M. supervised the project. All authors have approved the final manuscript.

Competing Interests

Patent application for the described antibody was filed by the Israel Institute for Biological Research. None of the authors declared any additional competing interests.

References

- 1 Corti, D. *et al.* Prophylactic and postexposure efficacy of a potent human monoclonal antibody against MERS coronavirus. *Proc Natl Acad Sci U S A* **112**, 10473-10478, doi:10.1073/pnas.1510199112 (2015).
- 2 Rockx, B. *et al.* Structural basis for potent cross-neutralizing human monoclonal antibody protection against lethal human and zoonotic severe acute respiratory syndrome coronavirus challenge. *J Virol* **82**, 3220-3235, doi:10.1128/JVI.02377-07 (2008).
- 3 Zhu, Z. *et al.* Potent cross-reactive neutralization of SARS coronavirus isolates by human monoclonal antibodies. *Proc Natl Acad Sci U S A* **104**, 12123-12128, doi:10.1073/pnas.0701000104 (2007).
- 4 Chen, Z. *et al.* Human Neutralizing Monoclonal Antibody Inhibition of Middle East Respiratory Syndrome Coronavirus Replication in the Common Marmoset. *J Infect Dis* **215**, 1807-1815, doi:10.1093/infdis/jix209 (2017).
- 5 Scheid, J. F. *et al.* Broad diversity of neutralizing antibodies isolated from memory B cells in HIV-infected individuals. *Nature* **458**, 636-640, doi:10.1038/nature07930 (2009).
- 6 Cohen, J. Antibodies may curb pandemic before vaccines. *Science* **369**, 752-753, doi:10.1126/science.369.6505.752 (2020).
- 7 Ju, B. *et al.* Human neutralizing antibodies elicited by SARS-CoV-2 infection. *Nature* **584**, 115-119, doi:10.1038/s41586-020-2380-z (2020).
- 8 Liu, L. *et al.* Potent neutralizing antibodies against multiple epitopes on SARS-CoV-2 spike. *Nature* **584**, 450-456, doi:10.1038/s41586-020-2571-7 (2020).
- 9 Yuan, M. *et al.* Structural basis of a shared antibody response to SARS-CoV-2. *Science* **369**, 1119-1123, doi:10.1126/science.abd2321 (2020).
- 10 Zost, S. J. *et al.* Potently neutralizing and protective human antibodies against SARS-CoV-2. *Nature* **584**, 443-449, doi:10.1038/s41586-020-2548-6 (2020).
- 11 Noy-Porat, T. *et al.* A panel of human neutralizing mAbs targeting SARS-CoV-2 spike at multiple epitopes. *Nat Commun* **11**, 4303, doi:10.1038/s41467-020-18159-4 (2020).
- 12 Baum A *et al.* REGN-COV2 antibodies prevent and treat SARS-CoV-2 infection in rhesus macaques and hamsters. *science* **Oct 9**, doi: 10.1126/.abe2402. (2020).
- 13 Mor M *et al.* Multi-Clonal Live SARS-CoV-2 In Vitro Neutralization by Antibodies Isolated from Severe COVID-19 Convalescent Donors. *BioRxiv*, doi: <https://doi.org/10.1101/2020.10.06.323634> (2020).
- 14 Tortorici, M. A. *et al.* Ultrapotent human antibodies protect against SARS-CoV-2 challenge via multiple mechanisms. *Science*, doi:10.1126/science.abe3354 (2020).
- 15 Johansen, M. D. *et al.* Animal and translational models of SARS-CoV-2 infection and COVID-19. *Mucosal Immunol*, doi:10.1038/s41385-020-00340-z (2020).
- 16 Bao, L. *et al.* The pathogenicity of SARS-CoV-2 in hACE2 transgenic mice. *Nature* **583**, 830-833, doi:10.1038/s41586-020-2312-y (2020).
- 17 Dinno, K. H., 3rd *et al.* A mouse-adapted model of SARS-CoV-2 to test COVID-19 countermeasures. *Nature*, doi:10.1038/s41586-020-2708-8 (2020).
- 18 Golden, J. W. *et al.* Human angiotensin-converting enzyme 2 transgenic mice infected with SARS-CoV-2 develop severe and fatal respiratory disease. *JCI Insight*, doi:10.1172/jci.insight.142032 (2020).
- 19 Hassan, A. O. *et al.* A SARS-CoV-2 Infection Model in Mice Demonstrates Protection by Neutralizing Antibodies. *Cell* **182**, 744-753 e744, doi:10.1016/j.cell.2020.06.011 (2020).
- 20 Jiang, R. D. *et al.* Pathogenesis of SARS-CoV-2 in Transgenic Mice Expressing Human Angiotensin-Converting Enzyme 2. *Cell* **182**, 50-58 e58, doi:10.1016/j.cell.2020.05.027 (2020).
- 21 Letko, M., Marzi, A. & Munster, V. Functional assessment of cell entry and receptor usage for SARS-CoV-2 and other lineage B betacoronaviruses. *Nat Microbiol* **5**, 562-569, doi:10.1038/s41564-020-0688-y (2020).

- 22 Lutz, C., Maher, L., Lee, C. & Kang, W. COVID-19 preclinical models: human angiotensin-converting enzyme 2 transgenic mice. *Hum Genomics* **14**, 20, doi:10.1186/s40246-020-00272-6 (2020).
- 23 Moreau, G. B. *et al.* Evaluation of K18-hACE2 Mice as a Model of SARS-CoV-2 Infection. *Am J Trop Med Hyg* **103**, 1215-1219, doi:10.4269/ajtmh.20-0762 (2020).
- 24 Sun, J. *et al.* Generation of a Broadly Useful Model for COVID-19 Pathogenesis, Vaccination, and Treatment. *Cell* **182**, 734-743 e735, doi:10.1016/j.cell.2020.06.010 (2020).
- 25 Wan, Y., Shang, J., Graham, R., Baric, R. S. & Li, F. Receptor Recognition by the Novel Coronavirus from Wuhan: an Analysis Based on Decade-Long Structural Studies of SARS Coronavirus. *J Virol* **94**, doi:10.1128/JVI.00127-20 (2020).
- 26 Winkler, E. S. *et al.* SARS-CoV-2 infection of human ACE2-transgenic mice causes severe lung inflammation and impaired function. *Nat Immunol*, doi:10.1038/s41590-020-0778-2 (2020).
- 27 Zheng, J. *et al.* K18-hACE2 Mice for Studies of COVID-19 Treatments and Pathogenesis Including Anosmia. *bioRxiv*, doi:10.1101/2020.08.07.242073 (2020).
- 28 Alsoussi, W. B. *et al.* A Potently Neutralizing Antibody Protects Mice against SARS-CoV-2 Infection. *J Immunol* **205**, 915-922, doi:10.4049/jimmunol.2000583 (2020).
- 29 Case, J. B. *et al.* Neutralizing Antibody and Soluble ACE2 Inhibition of a Replication-Competent VSV-SARS-CoV-2 and a Clinical Isolate of SARS-CoV-2. *Cell Host Microbe*, doi:10.1016/j.chom.2020.06.021 (2020).
- 30 Rogers, T. F. *et al.* Isolation of potent SARS-CoV-2 neutralizing antibodies and protection from disease in a small animal model. *Science* **369**, 956-963, doi:10.1126/science.abc7520 (2020).
- 31 Dall'Acqua, W. F., Cook, K. E., Damschroder, M. M., Woods, R. M. & Wu, H. Modulation of the effector functions of a human IgG1 through engineering of its hinge region. *J Immunol* **177**, 1129-1138, doi:10.4049/jimmunol.177.2.1129 (2006).
- 32 Gaudinski, M. R. *et al.* Safety and pharmacokinetics of the Fc-modified HIV-1 human monoclonal antibody VRC01LS: A Phase 1 open-label clinical trial in healthy adults. *PLoS Med* **15**, e1002493, doi:10.1371/journal.pmed.1002493 (2018).
- 33 Oganessian, V. *et al.* Structural insights into neonatal Fc receptor-based recycling mechanism. *The Journal of Biological Chemistry* **289**, 7812-7824 (2014).
- 34 Yu, X. Q. *et al.* Safety, Tolerability, and Pharmacokinetics of MEDI4893, an Investigational, Extended-Half-Life, Anti-Staphylococcus aureus Alpha-Toxin Human Monoclonal Antibody, in Healthy Adults. *Antimicrob Agents Chemother* **61**, doi:10.1128/AAC.01020-16 (2017).
- 35 Noy-Porat, T. *et al.* Acetylcholinesterase-Fc Fusion Protein (AChE-Fc): A Novel Potential Organophosphate Bioscavenger with Extended Plasma Half-Life. *Bioconjug Chem* **26**, 1753-1758, doi:10.1021/acs.bioconjchem.5b00305 (2015).
- 36 Jia, H., Yue, X. & Lazartigues, E. ACE2 mouse models: a toolbox for cardiovascular and pulmonary research. *Nat Commun* **11**, doi:<https://doi.org/10.1038/s41467-020-18880-0> (2020).
- 37 Noy-Porat, T. *et al.* Extended therapeutic window for post-exposure treatment of ricin intoxication conferred by the use of high-affinity antibodies. *Toxicon* **127**, 100-105, doi:10.1016/j.toxicon.2017.01.009 (2017).
- 38 Rosenfeld, R. *et al.* Isolation and chimerization of a highly neutralizing antibody conferring passive protection against lethal Bacillus anthracis infection. *PLoS One* **4**, e6351, doi:10.1371/journal.pone.0006351 (2009).
- 39 Lee, W. S., Wheatley, A. K., Kent, S. J. & DeKosky, B. J. Antibody-dependent enhancement and SARS-CoV-2 vaccines and therapies. *Nat Microbiol* **5**, 1185-1191, doi:10.1038/s41564-020-00789-5 (2020).
- 40 Yahalom-Ronen, Y. *et al.* A single dose of recombinant VSV-ΔG-spike vaccine provides protection against SARS-CoV-2 challenge *bioRxiv*, doi:10.1101/2020.06.18.160655 (2020).